

Article

The Accumulation of Metal Ions by a Soy Protein–Inorganic Composite Material

Masanori Yamada ^{1,*}, Maika Ujihara ¹ and Tetsuya Yamada ²

¹ Department of Chemistry, Faculty of Science, Okayama University of Science, Ridaicho, Kita-ku, Okayama 700-0005, Japan; ujihara.ous@gmail.com

² Graduate School of Agriculture, Hokkaido University, Kita 9, Nishi 9, Sapporo 060-8589, Hokkaido, Japan; tetsuyay@agr.hokudai.ac.jp

* Correspondence: myamada@ous.ac.jp

Abstract: Water-soluble soy protein (SP), which contains many acidic amino acids in its structure, was complexed by mixing with a silane coupling agent, 3-glycidioxypropyltrimethoxysilane (GPTMS). These SP–GPTMS composite materials showed stability in water. This property is due to the cross-linking between SP and GPTMS through the ring cleavage reaction of the epoxy group in the GPTMS molecule and an encapsulation of SP into the 3D siloxane network of GPTMS. When the SP–GPTMS composite material was immersed in an aqueous Cu(II) ion solution, the composite material changed from light brown to blue green by the coordination of Cu(II) ions into the SP. Hence, we evaluated the accumulation of heavy ions, rare-earth ions, and light metal ions. The accumulating affinity of metal ions was Cd(II) << Zn(II), Cu(II), Pb(II) < La(III) < Al(III) < Nd(III), In(III) << Mg(II) < Ca(II) ions. In addition, the sorption capacities of Ca(II), Mg(II), In(III), Nd(III), Al(III), La(III), Pb(II), Cu(II), Zn(II), and Cd(II) ions were 700 nmol/mg, 660 nmol/mg, 470 nmol/mg, 470 nmol/mg, 410 nmol/mg, 380 nmol/mg, 350 nmol/mg, 350 nmol/mg, 300 nmol/mg, and 200 nmol/mg, respectively. These properties suggest that the SP–GPTMS composite material has a divalent light metal ion selectivity. Additionally, the accumulative mechanism of the light metal ions was related to the carboxylate group and the hydroxyl group in the composite material.

Keywords: water-soluble soy protein; accumulation; metal ion; acidic amino acid; biopolymer–inorganic composite material; environmental material



Citation: Yamada, M.; Ujihara, M.; Yamada, T. The Accumulation of Metal Ions by a Soy Protein–Inorganic Composite Material. *J. Compos. Sci.* **2023**, *7*, 419. <https://doi.org/10.3390/jcs7100419>

Academic Editor: Francesco Tornabene

Received: 22 August 2023

Revised: 14 September 2023

Accepted: 25 September 2023

Published: 7 October 2023



Copyright: © 2023 by the authors. Licensee MDPI, Basel, Switzerland. This article is an open access article distributed under the terms and conditions of the Creative Commons Attribution (CC BY) license (<https://creativecommons.org/licenses/by/4.0/>).

1. Introduction

Soybean is eaten around the world. In Japan, especially, soybeans are eaten as traditional foods, such as in miso, soy sauce, tofu, tofu skin, natto, etc. Recently, these high-protein and low-calorie foods made from soybeans have attracted attention as health foods. In contrast, since soybean contains approximately 20% fat, such as linoleic acid or oleic acid, by dried weight [1,2], soybeans are cultivated all over the world for their oil. The production amount of soybean oil was ca. 60 million tons in 2021 [3]. These soybean oils are used as cooking oils, industrial oils, bio-fuel, chemical agents, and soy ink [4–6]. The degreased soybean, which is soybean after the oil extraction, contains a large amount of protein. Therefore, soy protein is used as a food for human consumption, livestock feed, fertilizer, etc. However, since the amount of degreased soybean is too large to use as a material, most degreased soybeans are discarded as industrial waste. In addition, soy protein is environmentally benign and a nonhazardous polymer. Therefore, these materials using soy protein have mainly been reported in the biological fields [7–9]. As an example outside the biological fields, we also reported a novel biodegradable bioplastic consisting of soy protein [10]. Furthermore, since the water-soluble soy protein contains many acidic amino acids with the carboxyl group on the side chains, such as aspartic acid (Asp) and glutamic acid (Glu), we reported that soy protein functions as an anhydrous proton conductor at intermediated temperature [11]. These negatively charged carboxylate

groups can interact not only with the positively charged protons, but also with various positively charged metal ions, such as light, heavy, and rare-earth metal ions, through the electrostatic interaction. Therefore, water-soluble soy protein might be used as a metal ion absorbent.

Industrial wastewater contains various metal ions. Such wastewater sometimes flows into river water and pollutes the environment. In addition, these metal ions may adversely affect the human body [12,13]. Therefore, the accumulation and removal of metal ions from industrial wastewater, river water, and ground water is a worldwide agenda [14]. The accumulation and removal of metal ions is mainly carried out using activated carbon and alumina. Although these absorbents, such as activated carbon and alumina, are low-cost materials, they do not possess any metal ion selectivity. In contrast, although polymer materials, such as ion-exchange resins, show a metal ion selectivity, they are expensive to synthesize. Additionally, the synthesized resins, which are made from petroleum as a raw material, burdens the environment. Therefore, the accumulation and removal of metal ions using biopolymers, such as polysaccharide, protein, and DNA, has been reported [15–19]. A biopolymer, which is synthesized in the natural world, is an environmentally benign material and can be easily disposed of after use. In particular, the accumulation of metal ions consisting of polysaccharides that are easy to purify and have a high molecular weight, such as cellulose, alginic acid, and chitosan, has been reported [15–18]. Recently, we also showed the selective accumulation of heavy metal and rare-earth metal ions using a polysaccharide, such as gellan gum or fucoidan [20,21]. The absorbance of metal ions using a biopolymer has mainly been reported for polysaccharides, and the utilization of protein is rarely reported. This is because it is difficult to obtain large amounts of protein. Therefore, we focused on water-soluble soy protein, which is environmentally benign, low cost, nonhazardous, and can be obtained from industrial waste.

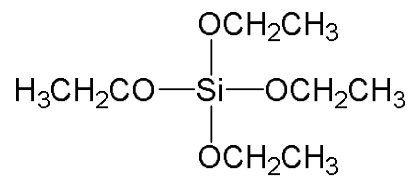
In order to use biopolymers as absorbents of metal ions, it is necessary to insolubilize the water-soluble soy protein. The insolubilization of a water-soluble protein includes its immobilization on a substrate, cross-linking, encapsulation, etc. However, the insolubilization of protein induces structural destruction and consequently decreases the functions that the protein possesses. In contrast, the organic–inorganic composite materials produced using a sol-gel process do not induce the functional deterioration of organic molecules. Therefore, organic–inorganic composite materials have been used for the insolubilization of an organic polymer, polysaccharide, and protein [20–25]. Recently, we reported the insolubilization of water-soluble polysaccharides, nucleic acids, and proteins by an organic–inorganic composite [20,21]. These biopolymer–inorganic composite materials with the function of a biopolymer have showed potential as an environmental material, such as through the absorbance of harmful organic compounds, carcinogenic compounds, and metal ions. Therefore, the soy protein–inorganic composite material, which was an insolubilized water-soluble soy protein produced using the sol-gel method, might be used as an absorbent of harmful compounds. To our knowledge, no organic–inorganic composite material using such water-soluble soy protein has been reported. Furthermore, there has been no report on the production of environmental materials such as metal ion adsorbents using water-soluble soy protein.

In this study, we prepared a soy protein–inorganic composite material by mixing the water-soluble soy protein (SP) and 3-glycidypropyltrimethoxysilane (GPTMS). This SP–GPTMS composite material showed water stability and thermal stability. Additionally, the SP–GPTMS composite material showed metal ion accumulative properties. The sorption capacities of Ca(II), Mg(II), In(III), Nd(III), Al(III), La(III), Pb(II), Cu(II), Zn(II), and Cd(II) ions were 700 nmol/mg, 660 nmol/mg, 470 nmol/mg, 470 nmol/mg, 410 nmol/mg, 380 nmol/mg, 350 nmol/mg, 350 nmol/mg, 300 nmol/mg, and 200 nmol/mg, respectively. These results suggest that the SP–GPTMS composite has selectivity for light metal ions such as Ca(II) ions and Mg(II) ions. The metal ion binding sites of the SP-GPS complex material were related to the carboxylate group and the hydroxyl group.

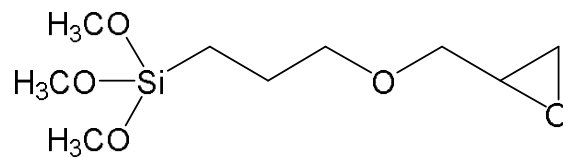
2. Materials and Methods

2.1. Material

Soy protein (SP), tetraethoxysilane (TEOS), 3-glycidoxypropyltrimethoxysilane (GPTMS), organic solvents, and hydrochloric acid were purchased from Fujifilm Wako Pure Chemical Industries, Osaka, Japan or Tokyo Kasei Industries, Tokyo, Japan. These agents were used without purification. Scheme 1a,b show the molecular structures of TEOS and GPTMS, respectively. The metal chlorides, such as $\text{CaCl}_2 \cdot 2\text{H}_2\text{O}$, $\text{MgCl}_2 \cdot 6\text{H}_2\text{O}$, $\text{AlCl}_3 \cdot 6\text{H}_2\text{O}$, $\text{InCl}_3 \cdot 4\text{H}_2\text{O}$, $\text{NdCl}_3 \cdot 6\text{H}_2\text{O}$, $\text{LaCl}_3 \cdot 7\text{H}_2\text{O}$, PbCl_2 , $\text{CuCl}_2 \cdot 2\text{H}_2\text{O}$, ZnCl_2 , and $\text{CdCl}_2 \cdot 2.5\text{H}_2\text{O}$, were obtained from Fujifilm Wako or Kanto Chemical Co., Tokyo, Japan. The standard solution of metal ions was purchased from Fujifilm Wako. Xylenol orange (XO), 4-(2-pyridylazo)resorcinol (PAR), and methylthymol blue (MTB) were obtained from Dojindo Co., Kumamoto, Japan or Fujifilm Wako. Ultrapure water was used in this experiment.



(a)



(b)

Scheme 1. Molecular structure of (a) TEOS and (b) GPTMS.

2.2. Preparation of the SP–GPTMS Composite Material

Water-soluble SP was obtained using the following procedure. The purchased soy protein was suspended in water (100 mg/mL) and stirred for a few hours. This solution was centrifuged to remove the water-insoluble components. The supernatant in which SP was dissolved was freeze-dried for 2 days or more. The composition values of amino acids contained in water-soluble SP were determined using an amino acid analyzer [11].

The SP–GPTMS composite material was prepared as follows: the water-soluble SP was dissolved in water (500 μL , 100 mg/mL) and 0.1 M HCl solution (five drops) was added to solution. Additionally, TEOS (five drops) was added to this solution and the mixed solution was stirred at RT for 12 h to promote hydrolysis. Subsequently, the GPTMS solution was quickly added to the SP–TEOS mixed solution and stirred vigorously at the same time. Then, 100 μL of the SP–GPTMS mixed solution was cast on a Teflon[®] plate and this cast plate was heated at 80 °C for 35 min to react with GPS. The mixing ratio R (wt.%) of the SP and GPTMS in SP–GPS composite material was defined using Equation (1):

$$R = \frac{(\text{weight of GPTMS})}{(\text{weight of SP}) + (\text{weight of GPTMS})} \times 100 \quad (1)$$

where (weight of SP) means the weight of the SP. Similarly, (weight of GPTMS) is the weight of the GPTMS. The R values varied from 0 to 70 wt.%.

2.3. Water Stability of the SP–GPTMS Composite Material

The water stability of the SP–GPTMS composite material was evaluated from the eluted amount of SP–GPTMS composite material dissolved in water. The eluted amount of the SP–GPTMS composite material was determined as follows: [20,21] the weight of dried SP–GPTMS composite material was measured using a precision balance and immersed in 5 mL of ultrapure water at RT for 1–24 h. The immersed composite materials were dried at RT for 12 h and the weight of these sample was measured once more. The eluted amount (%) of SP–GPTMS composite material was determined by Equation (2):

$$\text{Eluted amount (\%)} = 100 - \frac{(\text{dried weight of composite material after immersion in water})}{(\text{dried weight of composite material})} \times 100 \quad (2)$$

where (dried weight of composite material) is the weight of dried SP–GPTMS composite material before immersion in water. Similarly, (dried weight of composite material after immersion in water) is the weight of dried SP–GPTMS composite material after immersion in water.

2.4. Structural Analysis of the SP–GPTMS Composite Material

The SP–GPTMS composite material was analyzed using IR spectrometry. A Fourier transform infrared spectrometer FT-IR 8400 (Shimadzu Corp., Kyoto, Japan) and FT/IR-4700 (JASCO Corporation, Tokyo, Japan) were used for spectrophotometry. The former was used for the KBr method. The latter was used for the attenuated total reflection (ATR) methods with the diamond ATR prism. These measurements were demonstrated at the resolution of 4 cm^{-1} .

2.5. Thermal Analysis of the SP–GPTMS Composite Material

The SP–GPTMS composite material was analyzed using thermogravimetric–differential thermal analysis (TG-DTA). The measuring equipment used was DTG-60 (Shimadzu Corp.). The measuring condition was a dry-nitrogen flow and the heating rate was $10 \text{ }^\circ\text{C min}^{-1}$. The normalization of the sample weight was performed at 1 mg.

2.6. Accumulation of Metal Ions by the SP–GPTMS Composite Material

Aqueous CaCl_2 , MgCl_2 , AlCl_3 , InCl_3 , NdCl_3 , LaCl_3 , PbCl_2 , CuCl_2 , ZnCl_2 , and CdCl_2 solutions were separately prepared by dissolving metal chloride in ultrapure water (0–100 ppm). One SP–GPTMS composite material was immersed in an aqueous metal ion solution (10 mL), stirred at RT for 6 h, and then the metal indicator (XO, MTB, or PAR) was added in a sample solution. This sample solution was analyzed using UV–Vis spectroscopy. The measuring equipment used was a diode array spectrophotometer U-0080D (Hitachi Co., Ltd., Tokyo, Japan) [20,21]. Since the absorbance of the metal ion with a metal indicator is proportional to the metal ion concentration, the accumulated amount was determined from the absorbance before and after immersion. In contrast, the absolute value of metal ions required for absolute measurement was estimated from a calibration curve prepared from the standard solution of each metal ion.

2.7. IR Measurements of Metal Ion-Accumulated SP–GPTMS Composite Material

The SP–GPTMS composite material was immersed in aqueous Ca(II) ion solutions (10 mL) of various concentrations at RT for more than 24 h. The obtained samples were washed with pure water and dried at RT for more than 12 h. The Ca(II) ion-accumulated SP–GPTMS composite materials were analyzed using an IR spectrometer with the ATR prism.

3. Results and Discussion

3.1. Preparation of the SP–GPTMS Composite Material

The SP–GPTMS mixed solution was obtained by mixing the SP, tetraethoxysilane (TEOS), and 3-glycidoxypropyltrimethoxysilane (GPTMS). Hydrochloric acid was used as a catalyst. This mixed solution was reacted at 80 °C for 35 min. The obtained SP–GPTMS composite material was a light brown film-like substrate. The SP–GPTMS without mixing the TEOS was brittle and could not produce films. In contrast, the SP material without the composite of GPTMS and the SP–GPTMS composite material without the heat treatment dissolved in water.

Figure 1 shows the eluted amount of (closed square) SP–30 wt.% GPTMS, (closed diamond) SP–40 wt.% GPTMS, (closed triangle) SP–50 wt.% GPTMS, and (closed circle) SP–60 wt.% GPTMS composite materials. Although the eluted amount of SP–GPTMS composite material showed a large value immediately after immersion in water, it reached a constant value at 2 h. In addition, the eluted amount of composite material was related to the mixing ratio of GPTMS and decreased as the GPTMS increased. In contrast, since the SP–20 wt.% GPTMS composite material did not show water stability, its water stability could not be measured. Additionally, the SP–70 wt.% composite material could not produce a film-like substrate. Hence, the SP–60 wt.% GPTMS composite material was used in subsequent experiments. Furthermore, since the water-soluble components affect the experiment results, these composite materials were stored in ultrapure water until they were used in the experiments.

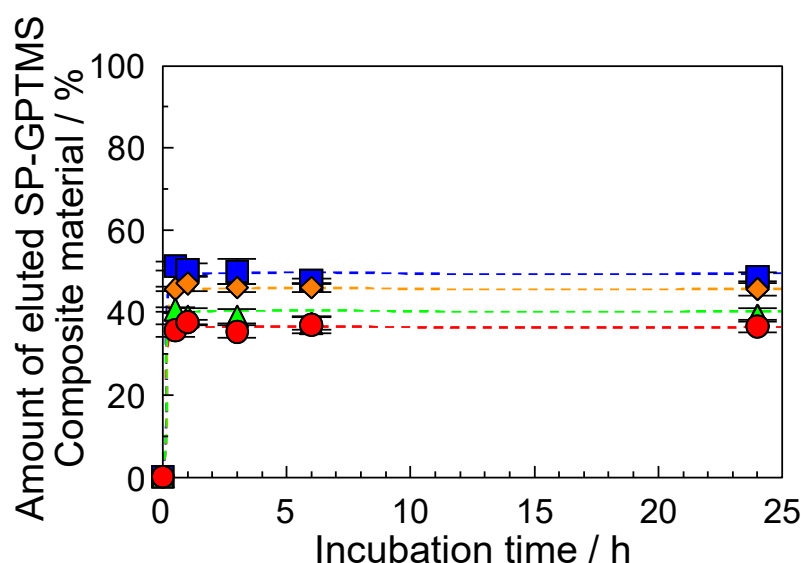


Figure 1. Eluted amount of SP–GPTMS composite material. (Closed square) SP–30 wt.% GPTMS, (closed diamond) SP–40 wt.% GPTMS, (closed triangle) SP–50 wt.% GPTMS, and (closed circle) SP–60 wt.% GPTMS composite materials. Each measuring value represents the average of three separate values \pm S.D.

3.2. Molecular Structure of the SP–GPTMS Composite Material

Generally, the Si–OCH₃ and Si–OCH₂CH₃ groups in the TEOS and GPTMS molecules, respectively, produce the silanol group through hydrolysis under acid conditions. These silanol groups further produce siloxanes through dehydration condensation [26]. In addition, the epoxy group in GPTMS and the hydroxyl group reacts through a ring cleavage reaction and produces ether bonding [27]. Figure 2 shows the IR spectra of (a) SP material without TEOS and GPTMS, (b) SP–60 wt.% GPTMS composite material, (c) TEOS material without the composite of GPTMS and SP, and (d) GPTMS material without TEOS and SP. The TEOS and GPTMS materials without the composite of SP showed a large absorption band at 1000–1100 cm^{−1}, which was related to the Si–O–Si stretching vibration.

The SP–60 wt.% GPTMS composite material also showed a similar large absorption band at 1000–1100 cm^{-1} . These results suggested that the SP material was encapsulated in the 3D network of Si–O–Si. Other biopolymer–inorganic composite materials [20,21] also showed similar phenomena, such as the encapsulation of a biopolymer into a 3D siloxane network. In addition, a GPTMS molecule with epoxy groups showed absorption bands at 820 cm^{-1} , attributed to C–O–C stretching vibrations with the distortion [28,29]. Although the SP–60 wt.% GPTMS composite material did not show absorption bands at 820 cm^{-1} , the absorption band at approximately 1070 cm^{-1} , with C–O–C stretching vibration without the distortion in ether [28–30], increased relatively. These results suggest that the epoxy group in the GPTMS and the hydroxyl group in SP reacted through the ring cleavage reaction of the epoxy group and produced the composite material with cross-linking.

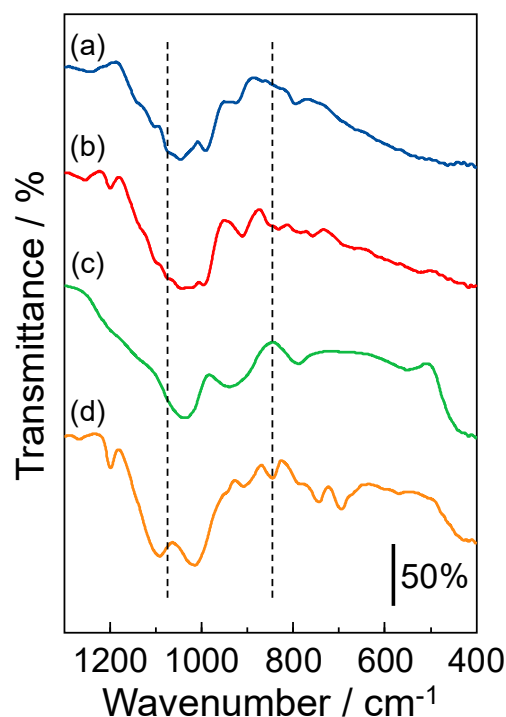


Figure 2. IR spectra of (a) SP without TEOS and GPTMS, (b) SP–60 wt.% GPTMS composite, (c) TEOS without the composite of GPTMS and SP, and (d) GPTMS without TEOS and SP. The TEOS and GPTMS samples were prepared using the heat treatment. Similar results were obtained in three experiments.

The TEOS material without GPTMS and SP showed the absorption bands at 930 cm^{-1} and 800 cm^{-1} , Si–OCH₂CH₃ and Si–OH bending vibrations, respectively. These absorption bands disappeared in the SP–GPTMS composite material. Additionally, GPTMS material without TEOS and SP showed the absorption band at 1220 cm^{-1} , with Si–CH₂ stretching vibration. A similar absorption band showed in the SP–GPTMS composite material. These results suggested that the hydrolysis reaction of silane coupling agents, such as TEOS and GPTMS, occurred sufficiently under our experimental condition. On the other hand, when the SP–GPTMS mixed solution without the addition of TEOS was cast onto a Teflon[®] plate, the dried material was brittle and did not form a film. In contrast, the composite material consisting of the gellan gum, one of the water-soluble anionic polysaccharides, and GPTMS formed a film without the addition of TEOS [20]. This was due to the difference in molecular structure. The SP and gellan gum have globular and linear structures, respectively. The gellan gum, which has long chains which intertwined with the siloxane network of GPTMS, formed a film without the addition of TEOS. The globular SP does not possess the long chain, like polysaccharide, and cannot intertwine with the siloxane network. As a result, the SP–GPTMS composite material without the addition of TEOS was brittle. In contrast,

since the GPTMS material with the addition of TEOS formed a longer siloxane network, SP was encapsulated into the siloxane network. Furthermore, since the GPTMS molecules formed cross-links with SP through the ring cleavage reaction of the epoxy group, SP was further stabilized within the siloxane network. Therefore, the water stability of SP–GPTMS composite material was increased by the composites through the sol-gel reaction.

3.3. Thermal Stability of the SP–GPTMS Composite Material

The TG-DTA measurement was demonstrated at a heating rate of $10\text{ }^{\circ}\text{C min}^{-1}$ under a dry-nitrogen flow. Figure 3a,b show TG and DTA of (1) the SP material without GPTMS and TEOS and (2) the SP–60 wt.% GPTMS composite material, respectively. The SP material without GPTMS and TEOS showed the large endothermic peak at $<100\text{ }^{\circ}\text{C}$, related to the evaporation of water. Consequently, the TG weight loss of SP material decreased. In addition, the exothermic peak at $>250\text{ }^{\circ}\text{C}$ also appeared. This peak was related to the thermal decomposition of SP material and the TG weight loss of the SP material further decreased. In contrast, although the SP–60 wt.% GPTMS composite material also showed an endothermic peak at $<50\text{ }^{\circ}\text{C}$ attributed to the evaporation of water, the large endothermic and exothermic peaks disappeared at $>100\text{ }^{\circ}\text{C}$. Consequently, the TG weight loss of the composite material was approximately 95% at $300\text{ }^{\circ}\text{C}$. The TG weight loss value of this composite material was smaller than that of the SP material. These results suggested that the encapsulation into a 3D siloxane network and the cross-linking through the ring cleavage reaction of the epoxy group provided thermal stability to the SP material.

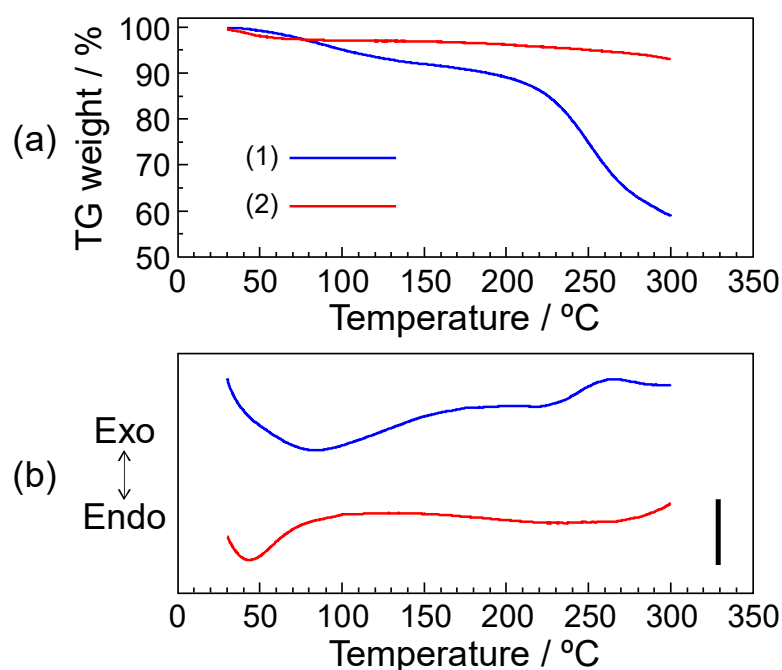


Figure 3. (a) TG and (b) DTA curves of (1) SP material without GPTMS and TEOS and (2) SP–60 wt.% GPTMS composite material. The TG-DTA measurements were demonstrated under a dry-nitrogen flow. Sample weights were normalized at 1 mg. A scale bar shows $5\text{ }\mu\text{V}$. Similar results were obtained in three experiments.

3.4. Accumulation of Metal Ions by the SP–GPTMS Composite Material

Since the water-soluble soy protein contains many acidic amino acids with the carboxyl group on the side chains, Asp and Glu, the SP–GPTMS composite material might be used as a metal ion absorbent. Therefore, we immersed the SP–GPTMS composite material in an aqueous Cu(II) ion solution. As a result, the composite material turned blue-green due to the coordination of the Cu(II) ions. These color changes have also been reported for other composite materials, such as a gellan gum–inorganic composite material [20]. In

addition, similar phenomena, such as color changes through the coordination of the metal ion, have also been reported for the Co(II) ion coordinated-alginate and -cellulose [31,32]. These results suggested that the SP–GPTMS composite material functions as a metal ion absorbent. In contrast, although the Cu(II) ion-accumulated SP–GPTMS composite was incubated in ultrapure water for 1 day, the composite material showed no bleaching by the release of Cu(II) ions.

Since many metal ions do not have absorption bands in the visible range, it is difficult to measure their concentrations using absorption spectroscopy. Therefore, metal indicators for the color agents are required to measure the concentration of metal ions. Figure 4 shows the relationship between the accumulated amounts of Cu(II) ions by the SP–GPTMS composite material and the incubation times. The aqueous Cu(II) ion solution with a concentration of 10 ppm was used. The accumulated amount of the Cu(II) ions increased with the incubation time and stopped changing at 6 h. The value at this time was approximately 220 nmol. A similar accumulating behavior was also obtained for other metal ions and the accumulated amount reached a constant value after a 6 h incubation time. Therefore, we evaluated the accumulation ability using the accumulated amount of metal ion at 6 h.

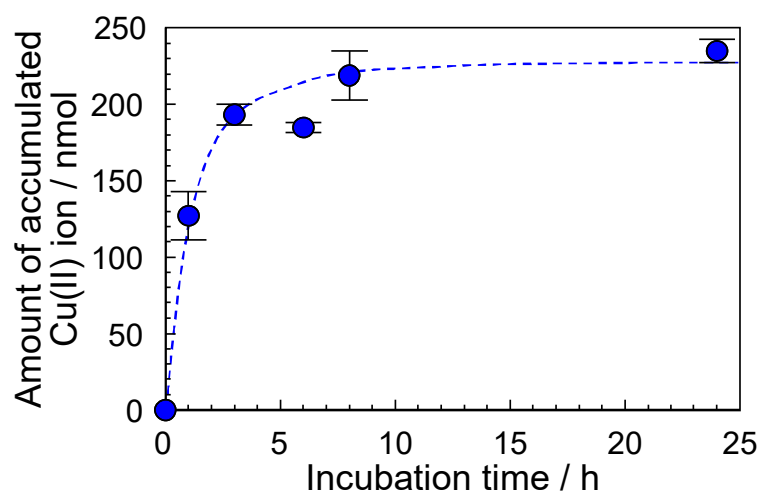


Figure 4. Accumulated amount of Cu(II) ion by the SP–60 wt.% GPTMS composite material at various incubation times. The Cu(II) ion concentration was 10 ppm. Each measuring value represents the average of three separate values \pm S.D.

The accumulated amounts of Cu(II), In(III), and Ca(II) ions at various concentrations are shown in Figure 5. The closed square, closed triangle, and closed circle indicate Cu(II), In(III), Ca(II) ions, respectively. The accumulated amount of the Cu(II) ions, which are among the heavy metal ions, increased with the increase in the initial concentration and stopped changing at approximately 400 ppm. This constant value was defined as the maximum accumulation amount of metal ions. Consequently, the maximum accumulated amount of the Cu(II) ions determined from a constant value was approximately 1.0 μ mol. This value was calculated from the average of three separate experiments. Similar accumulating behaviors were also obtained for In(III), which is one of the rare-earth metal ions, and Ca(II) ions, which are among the light metal ions. The maximum accumulated amounts of the In(III) and Ca(II) ions determined from a constant value were 1.5 μ mol and 2.2 μ mol, respectively, and these values were higher than for Cu(II) ions. Similar measurements were demonstrated for Al(III), Nd(III), La(III), Pb(II), Zn(II), and Cd(II) ions. Figure 6 shows the maximum accumulated amounts of 10 types of metal ions, which were calculated as a constant value which was obtained from the curve of the initial metal ion concentration versus the metal ion accumulation amount. The accumulating affinity of the SP–60 wt.% GPTMS composite material for metal ions was Cd(II) \ll Zn(II), Cu(II), Pb(II) $<$ La(III) $<$ Al(III) $<$ Nd(III), In(III) \ll Mg(II) $<$ Ca(II) ions. The accumulated amounts of Ca(II) and Mg(II) ions, which are classified as light metal ions, were more than 2.1 μ mol, and these

values were more than three times higher than those of the Cd(II) ions, which were the least accumulated metal ions in this experiment. On the other hand, the sorption capacity was calculated from the maximum accumulated amount of each metal ion. As a result, the sorption capacities of Ca(II), Mg(II), In(III), Nd(III), Al(III), La(III), Pb(II), Cu(II), Zn(II), and Cd(II) ions were 700 nmol/mg, 660 nmol/mg, 470 nmol/mg, 470 nmol/mg, 410 nmol/mg, 380 nmol/mg, 350 nmol/mg, 350 nmol/mg, 300 nmol/mg, and 200 nmol/mg, respectively. These results suggested that the SP–GPTMS composite material indicated light metal ion selectivity, such as for Ca(II) and Mg(II) ions.

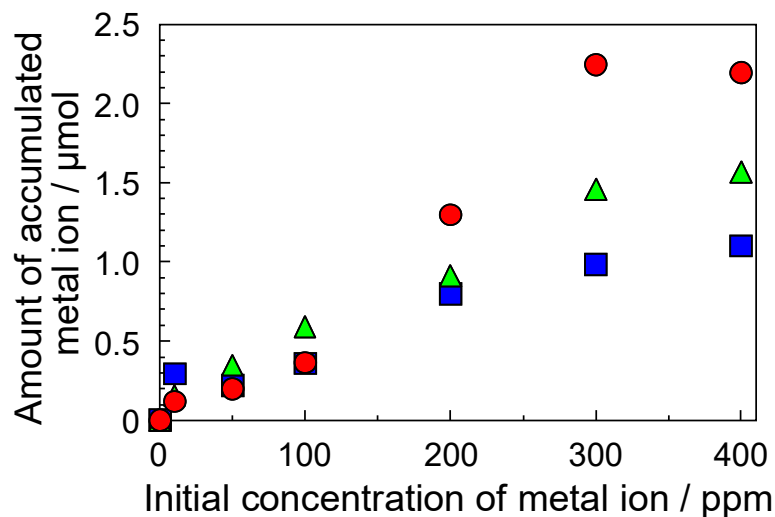


Figure 5. Accumulated amounts of (closed square) Cu(II), (closed triangle) In(III), and (closed circle) Ca(II) ions. These experiments were demonstrated at the incubation time of 6 h. Each value represents the mean of three separate determinations.

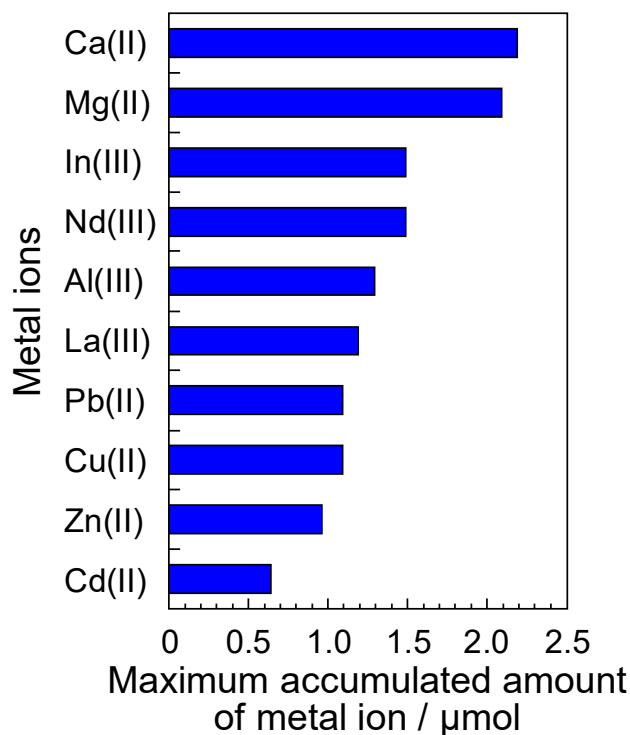


Figure 6. Maximum accumulated amounts of metal ions by the SP–GPTMS composite material. The maximum accumulated amount was calculated from a constant value which was obtained from the curve of initial metal ion concentration versus the metal ion accumulation amount.

3.5. IR Spectra of the Ca(II) Ion-Accumulated SP–GPTMS Composite Material

The SP–GPTMS composite material, which was immersed in an aqueous Ca(II) ion solution, was used for the IR sample. The IR spectra of the Ca(II) ion-accumulated SP–GPTMS composite from 400 to 1800 cm^{-1} are shown in Figure 7. The concentrations of aqueous Ca(II) ion solutions were (a) 0 ppm (immersed in ultrapure water), (b) 500 ppm, (c) 1000 ppm, (d) 2000 ppm, and (e) 4000 ppm. The SP–GPTMS composite material appeared to have an absorption band at 1535 cm^{-1} , with the symmetric stretching vibration of the carboxylate group [30,33,34]. This absorption band decreased when the Ca(II) ion concentration decreased. This is due to the electrostatic interaction between the Ca(II) ion and the carboxylate group. The fucoidan–inorganic composite also showed similar phenomena, such as the change in the absorption band by the interaction with charge [21]. In contrast, the absorption band of amide I at 1650 cm^{-1} [30] decreased when the Ca(II) ion concentration increased. These results suggested the conformational change in the protein structure by the accumulation of metal ions.

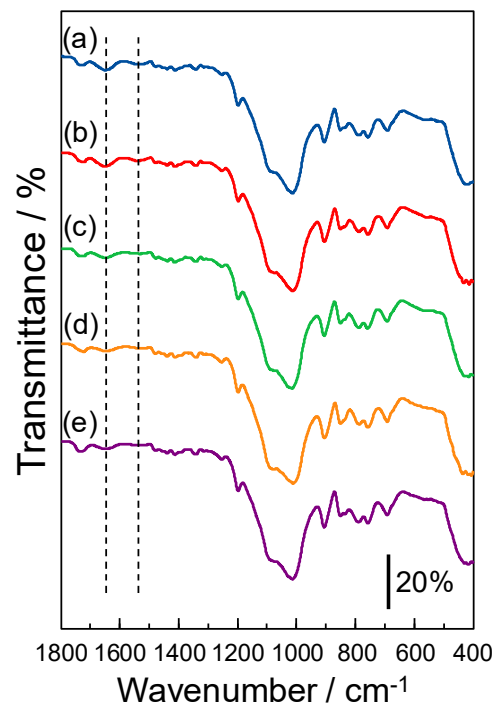


Figure 7. IR spectra of Ca(II) ion-accumulated SP–60 wt.% GPTMS composite material from 400 to 1800 cm^{-1} . The concentrations of aqueous Ca(II) ion solutions were (a) 0 ppm (immersed in ultrapure water), (b) 500 ppm, (c) 1000 ppm, (d) 2000 ppm, and (e) 4000 ppm. Similar results were obtained in three experiments.

The IR spectra of the Ca(II) ion-accumulated SP–GPTMS composite material from 2500 to 4000 cm^{-1} are shown in Figure 8. The concentrations of aqueous Ca(II) ion solutions were (a) 0 ppm (immersed in ultrapure water), (b) 500 ppm, (c) 1000 ppm, (d) 2000 ppm, and (e) 4000 ppm. The SP–GPTMS composite material showed an absorption band at approximately 3320 cm^{-1} , with O–H stretching vibration [30]. The water-soluble SP contained approximately 9% serine (Ser) and threonine (Thr), which possessed a hydroxyl group on the side chains in the amino acid components. In addition, the epoxy group in the GPTMS molecules produced the hydroxyl group via the ring cleavage reaction. This absorption band was shifted ca. 50 cm^{-1} to the higher wavenumber when the Ca(II) ion concentration increased. This phenomenon is due to the coordination of Ca(II) ions in the SP–GPTMS composite material. These phenomena suggested that the accumulation of metal ions occurred not only with the carboxylate group but also with the hydroxyl group.

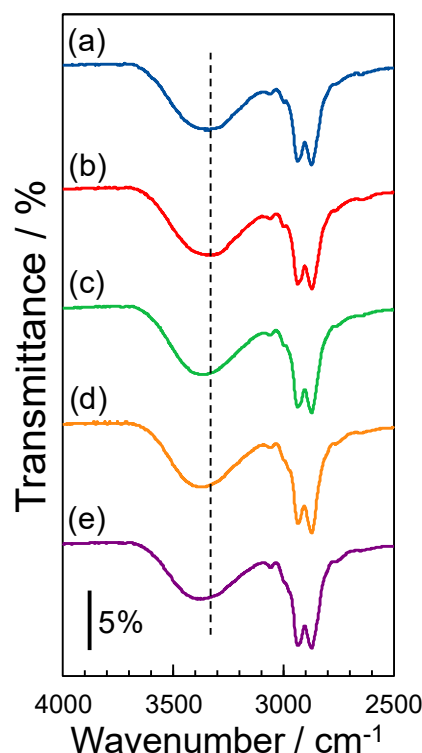


Figure 8. IR spectra of Ca(II) ion-accumulated SP–60 wt.% GPTMS composite material from 2500 to 4000 cm^{-1} . The concentrations of Ca(II) ions in an aqueous solution were (a) 0 ppm (immersed in ultrapure water), (b) 500 ppm, (c) 1000 ppm, (d) 2000 ppm, and (e) 4000 ppm. Similar results were obtained in three experiments.

3.6. Selective Mechanism of Metal Ions by the SP–GPTMS Composite Material

The SP–GPTMS composite materials selectively accumulated Ca(II) and Mg(II) ions, which are classified as divalent light metal ions. In addition, the IR spectra of the metal ion-accumulated composite material indicated that metal ions interacted with the carboxylate group and the hydroxyl group in the composite material. Generally, the strength and weakness of interactions between metal ions and functional groups have been discussed regarding the hard and soft acids and bases (HSAB) theory [35,36]. Therefore, we discussed the reason why the SP–GPTMS composite material selectively accumulated light metal ions using the HSAB theory and the ionic valence of metal ions.

In the HSAB theory, hard acids and soft acids strongly interact with hard bases and soft bases, respectively [35,36]. Generally, Ca(II) and Mg(II) ions, which are the divalent light metal ions, are classified as hard acids. Additionally, the carboxylate group and the hydroxyl group are classified as hard bases. The interaction based on the HSAB theory coincided with our experiments and the SP–GPTMS composite material showed the divalent light metal ion selectivity through the interaction between the divalent light metal ion and the carboxylate group and the hydroxyl group. In contrast, In(III), Nd(III), and La(III) ions were used in our accumulative experiment, and are classified as trivalent rare-earth ions. Additionally, these ions are also classified as hard acids. However, the atomic radius of rare earth ions is larger than that of divalent light metal ions, and the acidity in the HSAB theory is weaker than that of divalent light metal ions [35–37]. Consequently, the interaction between rare-earth ions and the composite material became smaller than the interaction with divalent light metal ions. In addition, the rare-earth ions used in our experiment were trivalent ions. In this case, since three anion sites accumulating trivalent ions were required and the coordination space for rare-earth ions increased, rare earth ions were less likely to be encapsulated in the 3D network of the SP–GPTMS composite material. Therefore, the accumulated amounts of the rare-earth ions were lower than those

of Ca(II) and Mg(II) ions. It is thought that the accumulated amount of Al(III) ion, which is one of the trivalent light metal ions and classified as a hard acid, also decreased for the same reason. On the other hand, Cu(II), Zn(II), Cd(II), and Pb(II) ions, which were used in our accumulative experiment, are classified as heavy metal ions. Additionally, according to the HSAB theory, these ions are classified as borderline acids [35,36]. The borderline acids do not interact strongly with hard bases, such as the carboxylate group and hydroxyl group. Consequently, the accumulated amounts of heavy metal ions were lower than those of the light metal and rare-earth ions. Therefore, the metal ion selectivity of the SP–GPTMS composite material was heavy metal ions < rare-earth and trivalent light metal ions < divalent light metal ions.

4. Conclusions

A water-insoluble SP–inorganic composite material was prepared by mixing the SP, GPTMS, and TEOS. The SP–GPTMS composite material effectively accumulated metal ions from the aqueous metal ion solution. The sorption capacities of Ca(II), Mg(II), In(III), Nd(III), Al(III), La(III), Pb(II), Cu(II), Zn(II), and Cd(II) ions were 700 nmol/mg, 660 nmol/mg, 470 nmol/mg, 470 nmol/mg, 410 nmol/mg, 380 nmol/mg, 350 nmol/mg, 350 nmol/mg, 300 nmol/mg, and 200 nmol/mg, respectively. Consequently, the SP–GPTMS composite material indicated selective accumulation for Ca(II) and Mg(II) ions, which are classified as divalent light metal ions. The soy protein is environmentally benign, low cost, non-hazardous, and can be obtained from industrial waste. Additionally, the soy protein is a sustainable resource for materials. Therefore, the SP–GPTMS composite material might be used as a water softener for drinking water, or in the removal of harmful metal ions from the body and to tackle the accumulation of valuable and expensive metal ions in industrial wastewater.

Author Contributions: Conceptualization, M.Y.; methodology, M.Y.; software, M.Y. and M.U.; validation, M.Y.; formal analysis, M.Y., M.U. and T.Y.; investigation, M.Y.; resources, M.Y.; data curation, M.Y., M.U. and T.Y.; writing—original draft preparation, M.Y.; writing—review and editing, M.Y.; visualization, M.Y.; supervision, M.Y.; project administration, M.Y.; funding acquisition, M.Y. All authors have read and agreed to the published version of the manuscript.

Funding: This research was funded by JSPS KAKENHI, grant number JP22K12451.

Data Availability Statement: All data generated or analyzed during this study are included in this published article.

Conflicts of Interest: The authors declare no conflict of interest.

References

1. Visakh, P.M.; Nazarenko, O. *Soy Protein-Based Blends, Composites and Nanocomposites*; John Wiley & Sons: Hoboken, NJ, USA, 1998.
2. El-Shemy, H. *Soybean Bio-Active Compounds*; IntechOpen Limited: London, UK, 2013.
3. Japan Oilseed Processors Association. Available online: <https://www.oil.or.jp/> (accessed on 1 August 2023).
4. Guo, B.; Sun, L.; Jiang, S.; Ren, H.; Sun, R.; Wei, Z.; Hong, H.; Luan, X.; Wang, J.; Wang, X.; et al. Soybean genetic resources contributing to sustainable protein production. *Theor. Appl. Genet.* **2022**, *135*, 4095–4121. [[CrossRef](#)] [[PubMed](#)]
5. Bhaskaran, S.K.; Boga, K.; Arukula, R.; Gaddam, S.K. Natural fibre reinforced vegetable-oil based polyurethane composites: A review. *J. Polym. Res.* **2023**, *30*, 325. [[CrossRef](#)]
6. Mori, R. Replacing all petroleum-based chemical products with natural biomass-based chemical products: A tutorial review. *RSC Sustain.* **2023**, *1*, 179–212. [[CrossRef](#)]
7. Vaz, C.M.; van Doeveren, P.F.N.M.; Reis, R.L.; Cunha, A.M. Soy matrix drug delivery systems obtained by melt-processing techniques. *Biomacromolecules* **2003**, *4*, 1520–1529. [[CrossRef](#)] [[PubMed](#)]
8. Vaz, C.M.; Fossen, M.; van Tuil, R.F.; de Graaf, L.A.; Reis, R.L.; Cunha, A.M. Casein and soybean protein-based thermoplastics and composites as alternative biodegradable polymers for biomedical applications. *J. Biomed. Mater. Res. A* **2003**, *65*, 60–70. [[CrossRef](#)]
9. Rani, S.; Kumar, R. A review on material and antimicrobial properties of soy protein isolate film. *J. Polym. Environ.* **2019**, *27*, 1613–1628. [[CrossRef](#)]
10. Yamada, M.; Morimitsu, S.; Hosono, E.; Yamada, T. Preparation of bioplastic using soy protein. *Int. J. Biol. Macromol.* **2020**, *149*, 1077–1083. [[CrossRef](#)]

11. Yamada, M.; Nagano, Y.; Yamada, T. Anhydrous proton conduction of soy protein. *Int. J. Electrochem. Sci.* **2021**, *16*, 151046. [[CrossRef](#)]
12. Bayuo, J.; Rwiza, M.J.; Sillanpää, M.; Mtei, K.M. Removal of heavy metals from binary and multicomponent adsorption systems using various adsorbents—A systematic review. *RSC Adv.* **2023**, *13*, 13052–13093. [[CrossRef](#)]
13. Aziz, K.H.H.; Mustafa, F.S.; Omer, K.M.; Hama, S.; Hamarawf, R.F.; Rahman, K.O. Heavy metal pollution in the aquatic environment: Efficient and low-cost removal approaches to eliminate their toxicity: A review. *RSC Adv.* **2023**, *13*, 17595–17610. [[CrossRef](#)]
14. Elbshary, R.E.; Gouda, A.A.; Sheikh, R.E.; Alqahtani, M.S.; Hanfi, M.Y.; Atia, B.M.; Sakr, A.K.; Gado, M.A. Recovery of W(VI) from wolframite ore using new synthetic Schiff base derivative. *Int. J. Mol. Sci.* **2023**, *24*, 7423. [[CrossRef](#)] [[PubMed](#)]
15. Dhir, B. Potential of biological materials for removing heavy metals from wastewater. *Environ. Sci. Pollut. Res.* **2014**, *21*, 1614–1627. [[CrossRef](#)] [[PubMed](#)]
16. Wang, J.; Chen, C. Biosorbents for heavy metals removal and their future. *Biotechnol. Adv.* **2009**, *27*, 195–226. [[CrossRef](#)]
17. Liu, C.; Liu, H.; Xiong, T.; Xu, A.; Pan, B.; Tang, K. Graphene oxide reinforced alginate/PVA double network hydrogels for efficient dye removal. *Polymers* **2018**, *10*, 835. [[CrossRef](#)] [[PubMed](#)]
18. Sakr, A.K.; Aal, M.M.A.; El-Rahem, K.A.A.; Allam, E.M.; Dayem, S.M.A.; Elshehy, E.A.; Hanfi, M.Y.; Alqahtani, M.S.; Cheira, M.F. Characteristic aspects of uranium(VI) adsorption utilizing nano-silica/chitosan from wastewater solution. *Nanomaterials* **2022**, *12*, 3866. [[CrossRef](#)] [[PubMed](#)]
19. Liu, X.D.; Yamada, M.; Matsunaga, M.; Nishi, N. Functional materials derived from DNA. *Adv. Polym. Sci.* **2007**, *209*, 149–178.
20. Yamada, M.; Kametani, Y. Preparation of gellan gum-inorganic composite film and its metal ion accumulation property. *J. Compos. Sci.* **2022**, *6*, 42. [[CrossRef](#)]
21. Yamada, M.; Shimanouchi, Y. Selective accumulation of rare-earth and heavy metal ions by a fucoidan-inorganic composite material. *Separations* **2022**, *9*, 219–229. [[CrossRef](#)]
22. Samiey, B.; Cheng, C.H.; Wu, J. Organic-inorganic hybrid polymers as adsorbents for removal of heavy metal ions from solutions: A review. *Materials* **2014**, *7*, 673–726. [[CrossRef](#)]
23. Sanchez, C.; Julián, B.; Belleville, P.; Popall, M. Applications of hybrid organic–inorganic nanocomposites. *J. Mater. Chem.* **2005**, *15*, 3559–3592. [[CrossRef](#)]
24. Pandey, S.; Mishra, S.B. Sol–gel derived organic–inorganic hybrid materials: Synthesis, characterizations and applications. *J. Sol-Gel Sci. Technol.* **2011**, *59*, 73–94. [[CrossRef](#)]
25. Ferreira, V.R.A.; Azenha, M.A.; Bustamante, A.G.; Mêna, M.T.; Moura, C.; Pereira, C.M.; Silva, A.F. Metal cation sorption ability of immobilized and reticulated chondroitin sulfate or fucoidan through a sol-gel crosslinking scheme. *Mater. Today Commun.* **2016**, *8*, 172–182. [[CrossRef](#)]
26. Plueddemann, E.P. *Silane Coupling Agents*, 2nd ed.; Plenum Press: New York, NY, USA, 1991.
27. Unnikrishnan, K.P.; Thachil, E.T. Toughening of epoxy resins. *Des. Monomers Polym.* **2006**, *9*, 129–152. [[CrossRef](#)]
28. Theophanides, T. *Infrared Spectroscopy—Materials Science, Engineering and Technology*; IntechOpen: London, UK, 2012.
29. Ma, S.; Liu, W.; Wei, Z.; Li, H. Mechanical and thermal properties and morphology of epoxy resins modified by a silicon compound. *J. Macromol. Sci. A* **2010**, *47*, 1084–1090. [[CrossRef](#)]
30. Silverstein, R.M.; Webster, F.X. *Spectrometric Identification of Organic Compounds*; John Wiley & Sons: New York, NY, USA, 1998.
31. Yajima, H.; Miyamoto, T.; Endo, R.; Furuya, S. Susceptibility of cobalt(II)-alginate complex films to moisture. *Kobunshi Ronbunshu* **1989**, *46*, 577–581. [[CrossRef](#)]
32. Boltinghouse, E.; Abel, K. Development of an optical relative humidity sensor. Cobalt chloride optical absorbency sensor study. *Anal. Chem.* **1989**, *61*, 1863–1866. [[CrossRef](#)]
33. Ptak, S.H.; Sanchez, L.; Fretté, X.; Kurouski, D. Complementarity of Raman and infrared spectroscopy for rapid characterization of fucoidan extracts. *Plant Methods* **2021**, *17*, 130. [[CrossRef](#)] [[PubMed](#)]
34. Shi, L.; Gunasekaran, S. Preparation of pectin–ZnO nanocomposite. *Nanoscale Res. Lett.* **2008**, *3*, 491–495. [[CrossRef](#)]
35. Ho, T.L. Hard soft acids bases (HSAB) principle and organic chemistry. *Chem. Rev.* **1975**, *75*, 1–20. [[CrossRef](#)]
36. Cotton, F.A.; Wilkinson, G.; Gaus, P.L. *Basic Inorganic Chemistry*; John Wiley & Sons: New York, NY, USA, 1991.
37. Ayers, P.W. The physical basis of the hard/soft acid/base principle. *Faraday Discuss.* **2007**, *135*, 161–190. [[CrossRef](#)]

Disclaimer/Publisher’s Note: The statements, opinions and data contained in all publications are solely those of the individual author(s) and contributor(s) and not of MDPI and/or the editor(s). MDPI and/or the editor(s) disclaim responsibility for any injury to people or property resulting from any ideas, methods, instructions or products referred to in the content.